International Journal of Automotive Technology, Vol. 6, No. 4, pp. 391–402 (2005)

1229-9138/2005/022-11

EFFECT OF BRAKE PEDAL IMPEDANCE ON BRAKING PERFORMANCE IN EH-BBW SYSTEM

S. PARK*

Department of Mechanical Engineering, Korea University, Seoul 136-713, Korea

(*Received 6 March 2004; Revised 13 January 2005*)

ABSTRACT–Despite its superior braking performance to conventional vehicles on test tracks, the performance of the ABS-equipped car seems disappointing on real highway. The poor braking performance results from questionable design of the human-machine interface (HMI) of the brake system. Force-displacement relation at the brake pedal has a strong effect on the braking performance. Recently developed brake-by-wire (BBW) system may allow us to tailor the force feel at the brake pedal. This study aims at exploring analytical ways of designing human-machine interface of BBW system. In this paper, mathematical models of brake pedal feel for electro-hydraulic BBW (EH-BBW) system are developed, and the braking motion and the characteristics of the driver's leg action are modeled. Based on the dynamic characteristics of the brake pedal and the driver, two new HMI designs for EH-BBW system are proposed. In the designs, BBW system is modeled as a type of master-slave teleoperator. The effectiveness of the proposed designs is investigated using driving simulation.

KEY WORDS : HMI (human-machine interface), Brake pedal impedance, BBW (brake-by-wire), Teleoperator

1. INTRODUCTION

Braking performance of modern vehicles has been greatly improved owing to the availability of powerful electronic components for antilock brake system (ABS) and stability control systems (Yu *et al.*, 2002). ABS provides the driver with an opportunity to steer out of emergencies by reducing the likelihood of wheel locking. The ABS, however, can save your life only if you know how to use it. Unfortunately, many drivers do not seem to understand how it should be operated. The accident statistics report that the implementation of ABS does not necessarily improve or could even impair the safety of drivers (Hertz *et al.*, 1995). The poor braking performance with ABS results from improper design of the human-machine interface (HMI) for the brake system; some drivers are confused by the vibration signal at the brake pedal indicating the normal activation of ABS (Yamaguchi, 1997).

Braking feel is determined by pedal force, pedal stroke, and vehicle deceleration (Ebert *et al.*, 1994; Sato *et al.*, 1996; Dairou *et al.*, 2003); the driver controls vehicle deceleration by sensing either brake pedal force or brake pedal stroke (or both of them) in addition to his visual and vestibular senses. Brake pedal feel (or brake pedal impedance) has great effects on perception of braking situation and, in turn, on braking performance. Conventionally, the brake pedal feel has been designed through trial and error on test tracks, where expert drivers evaluate the pedal feel of each brake system setup. This method requires a lot of time and cost and applies to the specific vehicle model only.

Recently, automotive industry has adopted the concept of "brake-by-wire" inspired by fly-by-wire (FBW) flight control (Kelling *et al.*, 2003). In FBW aircraft, bulky mechanical linkages have been replaced by wires, and there is no direct energy flow between the pilot and the mechanical system. Owing to electric signaling between the control input device and the actuator, the feel of the control device such as a control stick is artificially created. It has proven that carefully tailored mechanical characteristics (or force-displacement relations) of the control stick provide the pilot with comfort as well as better maneuverability. Automotive engineers are hoping for this improvement in "brake-by-wire" (BBW) controls of the automobile, where the control capabilities of electronic devices decouple the energetic interaction between the hydraulic line and the brake pedal and allow us to tailor the dynamic characteristics of the control unit. Sensors determine the driver's braking command and transmit this information to an electronic control unit. Using the corresponding actuators, the control unit creates the required brake effect on the wheels. Electro-Hydraulic Brake (EHB) uses hydraulic brake compo-

*Corresponding author. e-mail: drsspark@korea.ac.kr

nents, such as a pressure control valve, a pump and an accumulator. Electro-Mechanical Brake (EMB) employs an electric motor, gears, and ball screws, rather than hydraulic components.

This study considers new aspects in designing brake pedal impedance of BBW system, particularly of EHB. First, mathematical models of brake pedal impedance are developed and are confirmed through computer simulations. Based on the models, brake pedal force is formulated as a function of pedal stroke and its rate. The mechanical impedance of the brake pedal can be represented in the form of impedance surface, three-dimensional plot of pedal force, pedal stroke and its rate. Second, the mechanical characteristics of the driver's braking motion are modeled. Studies on human motor control suggest the driver's initial or emergency braking motion can be modeled as a preprogrammed action (Park, 1999). After considering the mechanical characteristics of brake system and the human driver, two novel human-machine interface designs of BBW system are proposed. The new designs employ the bilateral teleoperation concept rather than the unilateral control employed in conventional brake systems. Teleoperator studies report that force feedback to the operator and the adaptive change of impedance at the master port enhance teleoperation performance (Raju, 1988). In the proposed designs brake pedal stiffness is controlled depending on braking activation or road surface conditions. Thus, the adaptive change of the brake pedal stiffness is intended to provide the driver with intuitive cues of braking activation or of road surface conditions- a softer pedal for a wet/icy road and a stiffer pedal for a dry road. In addition the preprogrammed nature of emergency leg motions produces further depression of a soft brake pedal on a wet road, which is advantageous for ABS in an emergency situation on wet/icy roads.

Braking performance of these proposed HMI designs is evaluated using a driving simulator. Road condition awareness by the test drivers and situation adaptability by the driver-vehicle systems are used for braking performance evaluation. The performance of the two new HMI designs and conventional brake systems are compared.

2. MATHEMATICAL MODELING OF HUMAN-MACHINE SYSTEM IN BRAKING

There are various kinds of input devices to control machine systems. Joysticks, handgrips, levers, buttons, and pedals are conventional control input devices using hand or foot. The control input devices may be categorized based on how the control input is mapped into control output as follows:

- Position control
Control input mapped into position output (computer mouse);
- Rate control
Control input mapped into speed output (gas pedal);
- Acceleration control
Control input mapped into acceleration output (steering wheel, brake pedal).

Braking can be considered as an acceleration (or deceleration) control, since the position of the brake pedal or pedal force is mapped into a deceleration level of the vehicle. Force feel from the brake pedal is also important in perceiving braking situations. This pedal feel is determined by stiffness (or more generally impedance) of the brake pedal. This pedal impedance plays an important role in delivering the driver's intention to the brake system and in delivering its feedback to the driver. To produce a desired pedal displacement the driver must produce a force determined by the mechanical impedance of the brake pedal; to produce a desired force requires a particular displacement, also determined by the impedance.

While the braking task appears to be a simple action, some drivers still have troubles in manipulating the brake pedal, as can be seen from the accident statistics of ABS-equipped cars (Hertz *et al.*, 1995). The full characterization of human limb characteristics is applicable to the design of a variety of human-machine interfaces, such as a pedal, a joystick, and a steering wheel. In designing a brake pedal, the characteristics of human leg motion should be taken into account. However, little is known about the mechanisms of musculo-skeletal motor control in the driver's braking motion; few studies have investigated this operation (Jackson, 1997; Park, 1999).

2.1. Modeling of Brake Pedal Impedance

This section introduces modeling of a pedal feel emulator of EHB. Since there is no energetic interaction between the actuation unit and the stroke simulator in BBW system, brake pedal impedance can be determined by dynamic characteristics of pedal feel emulator only. Here,

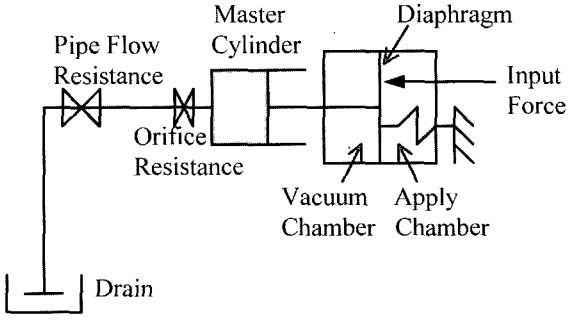

Figure 1. Stroke simulator with vacuum booster.

simplified mathematical models of pedal force for two different EHB systems are presented: pedal feel emulators with and without the vacuum booster.

2.1.1. Pedal feel emulator with vacuum booster

The hydromechanical type pedal feel emulator in Figure 1 consists of a vacuum booster, a master cylinder, and a linear pressure valve. The vacuum booster consists of two chambers (apply and vacuum chambers), a diaphragm between them, a push rod and a power piston, their return springs, a rubber reaction washer, and control valves.

In the vacuum booster, force balance in the push rod and the power piston yields the following equations (Gerdes *et al.*, 1999):

$$F_{out} = F_d + F_{in} - F_{rs} \tag{1}$$

where F_{out} and F_{in} represent the vacuum booster output and input forces. The force across diaphragm, F_d, is produced by pressure difference between two chambers:

$$F_d = A_d(P_a - P_v) \tag{2}$$

where $P_a = \dfrac{m_v RT}{V_{vo} - A_d x_{pp}}$ and $P_v = \dfrac{m_v RT}{V_{vo} - A_d x_{pp}}$. Here,

x_{pp} denotes the displacement of the power piston, R gas constant, T temperature, V_{a0} initial volume of apply chamber, and V_{v0} initial volume of vacuum chamber. Air masses in apply and vacuum chambers (m_a and m_v) are determined by dynamics of the engine and the powertrain. Here, the air masses in apply and vacuum chambers are assumed to be constant, and the temperature T is also assumed to be constant during the operation. These simplifications seem plausible in quick application of pedal force input.

The force in the return spring can be described as:

$$F_{rs} = F_{rs0} + K_{rs} x_{pp} \tag{3}$$

where F_{rs0} and K_{rs} represent preload and stiffness of the return spring, respectively.

The pressure in the master cylinder is described as

$$P_{mc} = \frac{F_{out} - F_{cs} - F_{cf}}{A_{mc}} \tag{4}$$

where F_{cs} and F_{cf} represent cylinder spring force and cylinder friction force, respectively. The cylinder spring force can be described as:

$$F_{cs} = F_{cs0} + K_{cs} x_{mc} \tag{5}$$

where F_{cs0} represents the preload in cylinder spring, K_{cs} stiffness of the cylinder spring, and x_{mc} displacement of the master cylinder piston.

The flow rate of brake oil out of the master cylinder is described as:

$$A_{mc}\dot{x}_{mc} = C_q\sqrt{P_{mc} - P_w} \tag{6}$$

where C_q represents the effective flow coefficient of the linear pressure valve and the hydraulic line. Here the master cylinder piston displacement x_{mc} is identical to the power piston displacement x_{pp} ($x_{mc} = x_{pp}$). If the brake oil flows into drain, the pressure in the wheel cylinder P_w is approximately zero.

Neglecting nonlinear Coulomb friction and airflow dynamics to and from the chambers in the vacuum booster, the force input at the brake pedal before the mechanical stop of the pedal can be described as:

$$F_{in} = L\left(-\frac{A_d m_v RT}{V_{v0} + A_d x} + \frac{A_d m_a RT}{V_{a0} - A_d x} + F_{cs0} + F_{rs0} - F_{cf} + (K_{cs} + K_{rs})x + R_p\dot{x} + \frac{A_{mc}^3\dot{x}^2}{C_q^2}\right) \tag{7}$$

where x represent the pedal stroke, L brake pedal leverage length ratio, and R_p flow resistance of the pipe. Note that the pedal force is a function of the pedal stroke and its time derivative. Results from numerical simulations of the developed model are presented and are compared with the experimental data. The experimental data was taken from the hydraulic brake pedal emulator. The data consists of pedal stroke, speed and acceleration of pedal depression, and pedal force. From the data taken, parameters of the system can be estimated through the least square fit method. Vacuum booster input force F_{in} can be rewritten as:

$$F_{in} = -\frac{C_1}{C_2 + C_3 x} + \frac{C_4}{C_5 - C_3 x} + C_6 + C_7 x + C_8\dot{x} + C_9\dot{x}^2 \tag{8}$$

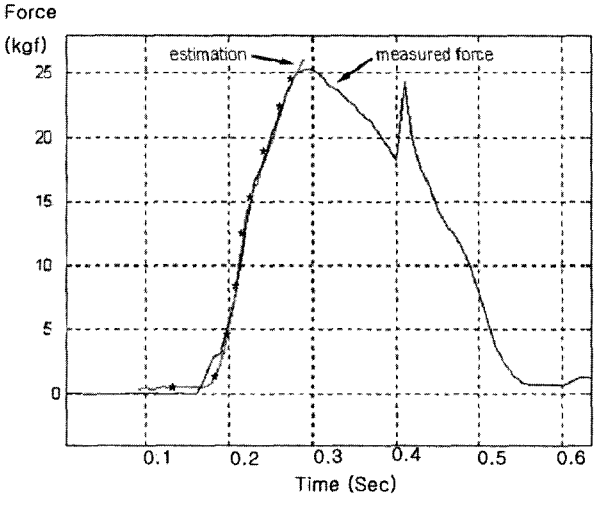

Figure 2. Measured and estimated pedal force for stroke simulator with vacuum booster (solid line: measured, dotted line: estimated).

With given F_{in}, x and $\dot{x}$, system parameters C_1 to C_9 can be estimated. Using the obtained parameters, brake force was estimated as shown in Figure 2. The model developed above is valid when pedal force is applied quickly as in emergency braking.

2.1.2. Pedal feel emulator without vacuum booster

This hydromechanical pedal feel emulator consists of a master cylinder, a proportional valve, and a slave cylinder (Figure 3). Neglecting nonlinear Coulomb friction and flow loss at the orifice, the force input to the brake pedal can be described as:

$$F_{in} = L\left[\left(K_m + K_w\frac{A_m^2}{A_w^2}\right)x + R_p A_m^2 \dot{x}\right] \tag{9}$$

where K_m and K_w represent the stiffnesses of the master cylinder spring and the slave cylinder spring, and A_m and A_w the areas of the master cylinder and the slave cylinder,

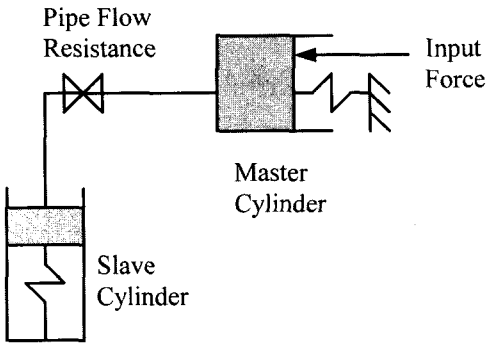

Figure 3. Stroke simulator without vacuum booster.

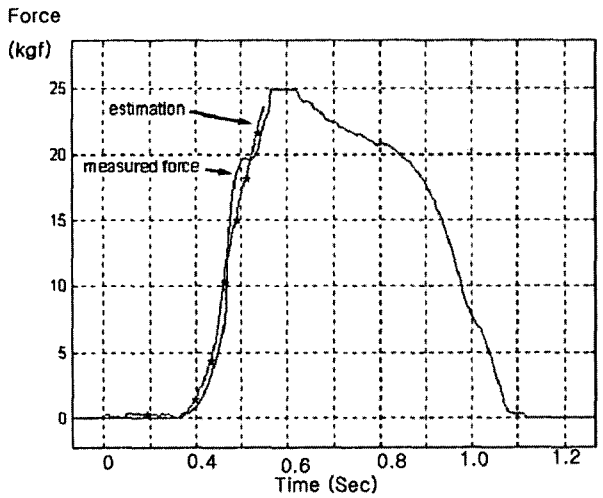

Figure 4. Measured and estimated pedal force for stroke simulator without a vacuum booster (solid line: measured, dotted line: estimated).

respectively. Note that the pedal force is a function of pedal stroke and its rate.

Results from numerical simulations of the developed models are presented and are compared with experimental data. The experimental data was taken from hydraulic stroke simulator. The data consists of pedal stroke, speed and acceleration of pedal depression, and pedal force. From the data taken, parameters of the system can be estimated through the least square fit method. The pedal input force F_{in} can be rewritten as:

$$F_{in} = C_1 x + C_2 \dot{x} \tag{10}$$

With given F_{in}, x, and $\dot{x}$, system parameters C_1 and C_2 can be estimated. Using the obtained parameters, brake force was estimated as shown in Figure 4.

2.1.3. Characterization of brake pedal impedance using impedance surface

In the previous sections, it is shown that mechanical impedance at the brake pedal can be determined through mathematical modeling of each component of the brake system, where the pedal force is formulated as a function of pedal stroke and its rate, but not of its acceleration. After determining model parameters using system identification, the impedance at the brake pedal can be presented in a three-dimensional plot. This may be called impedance surface, which describes relation among pedal force, pedal stroke and its rate. Figure 5 shows the impedance surface and measured data from a German passenger car (Audi A4). The figure shows that the measured data lies on the impedance surface, which was calculated from mathematical model. The plot clearly indicates the effect of damping as well as stiffness. In designing control device such as joystick, damping is usually added to smooth controlled output and stabilize the system performance.

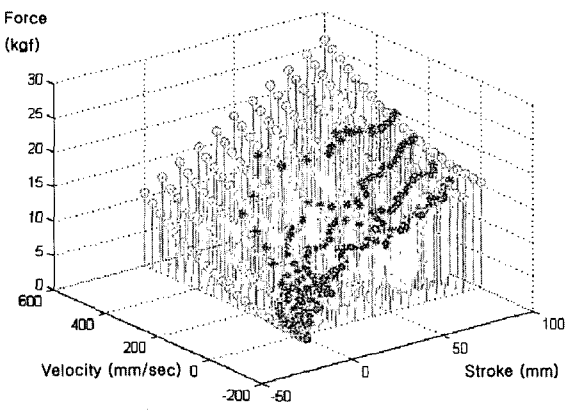

Figure 5. Impedance surface of brake pedal (*: measured data, o: impedance surface from mathematical model).

This impedance surface presented here may be used for pedal force control of the stroke simulator of BBW system. In designing BBW system, the map of the pedal force and the pedal stroke is usually used as a reference input to the pedal feel emulator. However, Figure 5 clearly shows that the force is a function of the stroke rate as well as the stroke. The impedance surface can be used as a map, which gives the desired pedal force as a function of pedal stroke and its rate. In BBW system, this map can be arbitrarily tailored thanks to decoupling between the brake actuation part and the stroke simulator. One possibility to design the impedance surface would be to benchmark brake systems of successful vehicle models. The map of "good" brake pedal feels may be acquired by measuring the pedal force, the pedal stroke and its speed from a brake system with a "good" braking feel.

2.2. Driver's Action on Brake Pedal

The driver controls the brake pedal in different manners in various braking situations. While every driver would take different action even in the same situation, all the braking actions may be categorized into two models. In *emergency* (or *initial*) *braking* situation, the driver press down on the pedal without the support at the heel and with no ankle action. In *normal braking* situation, the driver uses his ankle with the support at the heel. Considering the characteristics of conventional brake pedal, damping in pedal impedance may affect quick emergency braking action, while it has little effect on slow braking motion in normal braking.

A great number of studies have attempted to reveal the basic properties of the human neuromuscular control system, and yet were unable to explain how the desired movement can be translated into the muscle activity. Some of human limb movements, however, may be considered as a preprogrammed open-loop motion. Under equilibrium point control hypothesis, human leg motion can be modeled as a mass-spring-damper system with open-loop input command from the central nervous system (CNS) (Won *et al.*, 1995; Park, 1999). Figure 6 shows a simplified one-dimensional model of human limb motion. In this model the CNS fires a simple the kinematic command (smooth point-to-point command) to the musculo-skeletal system (a mass-spring-damper system) without feedback. With smooth CNS command with a symmetric speed profile (dotted line), the resulting movement of the limb (solid line) shows a smooth time-displacement curve with a asymmetric bell-shaped speed profile.

In his study on human leg motion, Park (1999) suggested that the *initial* braking action by the driver's leg can be modeled as follows:

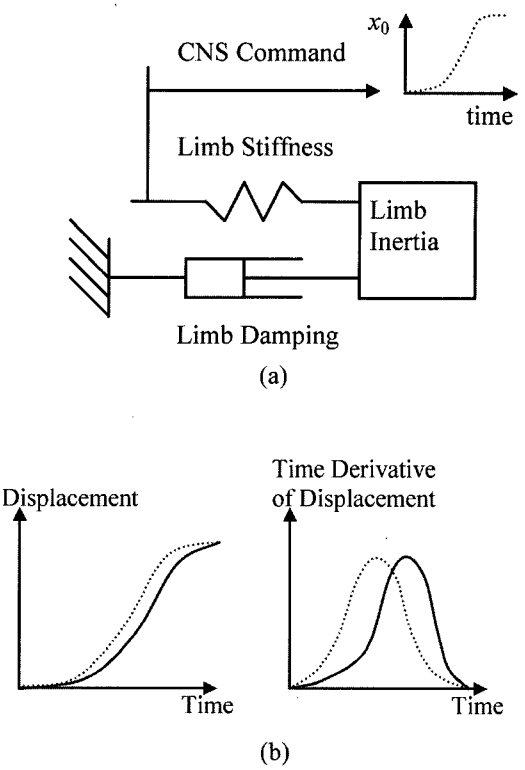

Figure 6. Human motor control model: (a) Mass-spring-damper model of human limb; (b) Human limb displacement (dotted line: CNS command, solid line: limb movement).

- Braking action is two-degree-of-freedom planar motion with free hip and knee joints.
- Braking action is a simple reaching motion by the foot with no visual target.
- In braking a movement in free space is followed by contact with the brake pedal.
- Braking action is a preprogrammed open-loop movement.

The preprogrammed braking action suggests the same motor command from the central nervous system (CNS)

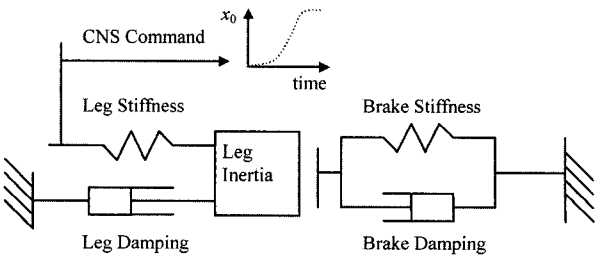

Figure 7. Driver-vehicle interface at brake pedal.

control movements both in free space and in contact with the brake pedal. It also implies the same motor commands for different brake pedal impedances; further pedal depression will be induced with a softer brake pedal with the same CNS command.

In Figure 7, driver-vehicle interface at the brake pedal is postulated with a simple driver leg model and brake system dynamics. According to equilibrium point control hypothesis of human motor control, braking motion can be modeled as a preprogrammed open-loop action. In the figure, motor command from the Central Nervous System (CNS) is depicted as x_0, which is a smooth function of time. While the maximum stroke we can get at the pedal is around 10 cm, the motor command x_0 (or driver's intention) in emergency braking would be much higher than the maximum pedal stroke. In normal braking situation, it would be less than 10 cm for fine control of braking force.

3. NEW HMI DESIGN FOR BBW SYSTEM

As discussed in the previous section, the brake pedal impedance or brake pedal feel has great effects on braking performance, as well as on perception of the braking situation. While it is generally acknowledged that brake pedal impedance greatly affects braking performance, there has been no analytical guideline on how they should be determined.

An automotive brake system can be considered to be a type of teleoperator rather than a simple open-loop manipulator; the foot-pedal interface can be modeled as a master port, and tire-road interface as a slave port. Force feedback in teleoperation can thereby be applied to the design of brake systems.

3.1. Modeling of BBW System as a Teleoperator

While control of brake systems is performed initially in an open-loop manner, conventional brake systems may be modeled as a teleoperator with poor performance feedback to the operator, where at the tire-road interface the braking task is performed by the *remote* driver using the brake pedal. If the brake system is modeled as a teleoperator (Figure 8), the braking task in an automobile is analogous to a contact task or to grabbing an object using a teleoperator. In grabbing an object using a teleoperator, the operator should apply enough force on the handgrip or joystick to achieve enough contact force between the manipulator and the task object. In a braking task using ABS, for example, the driver should apply enough force to the brake pedal to achieve enough braking force at tire-road contact. Keeping the maximum braking force in ABS can be considered as equivalent to keeping enough contact force with the task object in teleoperation. Upon activation of ABS, the tire-road contact achieves its firmest grip.

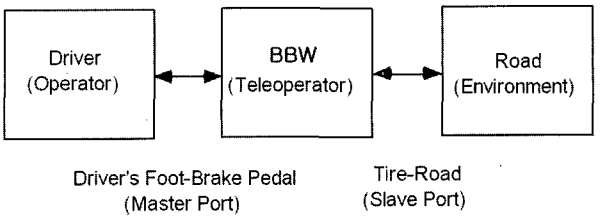

Figure 8. Brake system as a teleoperator.

In ABS, the signal indicating maximum braking is a non-intuitive vibration from the brake pedal; in teleoperation the force of contact with a task object can be sensed by force feedback to the operator. As noted earlier, it is believed that the signal for required force in ABS braking can be better achieved by a change of impedance at the master port, i.e., at the brake pedal.

While a visual or auditory signal may also be available, force feedback or kinesthetic display appears to be more promising in the braking task, since the driver's visual or auditory sense is usually occupied by other information. While most importance is typically placed on our visual sense of the environment, it is the kinesthetic sense that provides us with much of the information necessary to modify and manipulate the world around us. There is a fundamental difference between kinesthetic information and that of visual and auditory displays. The visual and auditory channels are unidirectional information flows, and they do not involve energetic interaction in the physical variables being sensed (Barfield *et al.*, 1995). In the kinesthetic channel a transfer of energy is involved, and this enables the joystick or brake pedal to serve as a *kinesthetic display* as well as an *input device.*

3.2. New BBW System Designs

In design of new HMI for BBW systems, two aspects are considered: the driver's braking motion and the modeling of the brake system as a teleoperator.

3.2.1. Proposed design 1

This system employs the ABS components, except that it has a servo system to change the pedal impedance while filtering out the pulsing of the pedal on ABS activation. Upon detection of wheel slippage by ABS sensors, the brake pedal is tuned to be softer. On a wet/icy road the driver can sense yielding of the pedal instead of vibration from it. If the braking motion of the driver is preprogrammed, a sudden change of the brake pedal impedance will induce further depression of the pedal, which is advantageous in ABS since full pedal depression induces ABS activation on a wet/icy road. This design is analogous to the teleoperator with adaptive impedance at

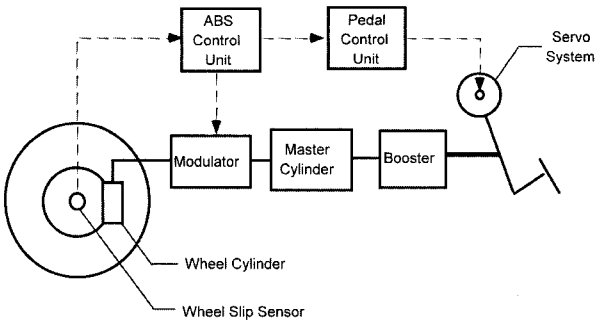

Figure 9. Schematic view of design 1.

the master port performing a contact task. For the teleoperator contact task, Raju (1988) suggested softer master impedance and stiffer slave impedance upon contact. This idea is directly applied to brake system design; upon activation of ABS, brake pedal impedance is tuned softer while tire-road contact gets firmer. Figure 9 illustrates this brake system design.

3.2.2. Proposed design 2

Current development of optoelectronic sensors allows us to detect the road surface condition as well as wheel slippage as in ABS. This sensor uses backscattered and reflected light information to detect the presence of ice, water, or mud on the road surface (Ciamberlini *et al.*, 1995). This new brake system employs the road surface sensor to control the brake pedal impedance in addition to the usual components of ABS, including the wheel slip sensor. In the proposed design upon detection of a wet/icy road, the impedance of the brake pedal is tuned softer. The driver is able to sense the road condition as he presses down on the pedal. This system is similar to a power steering wheel on an icy road; the steering wheel can be turned more easily on an icy road than on a dry road. This system depends on the correct sensing of road surface condition. Figure 10 illustrates this brake system design.

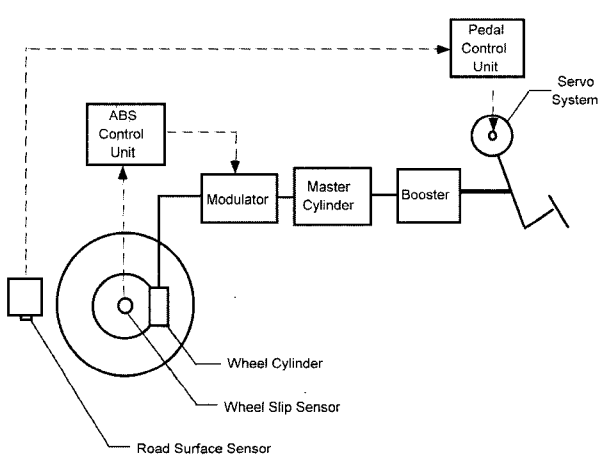

Figure 10. Schematic view of design 2.

Just as in conventional ABS, in the systems proposed above a further pedal depression after ABS activation makes no difference in the braking force. Rather the proposed systems lead the driver to full depression of pedal by softening the pedal stiffness when the maximum braking force is needed. Also, the driver can realize the road condition from the change in pedal stiffness.

4. DRIVING SIMULATOR TESTS

To test the applicability of the proposed designs, a driving simulator was developed for braking simulation.

4.1. Simulator System

The simulator developed for this study was a simplified version of a fixed-base driving simulator. The whole simulation system was under control of a PC-Pentium computer, which managed the hardware control, visual display, and braking situation sequence encountered by the driver.

The PC processed the brake pedal position or command signal by calculating vehicle and brake system dynamics to yield vehicle motion on a visual display, namely the relative size of an object representing a leading car. While an active gas pedal was not provided in the simulator (only a foot rest from where the test driver moved his foot to brake), the speed of the car was gradually accelerated back to the reference speed upon release of the brake pedal. A speedometer was also provided to indicate the speed of the driver car. All this information was displayed on the PC monitor screen in front of the driver. The screen was updated at about 20 frames/sec yielding the minimum smooth motion. To produce a relatively large brake pedal force, an AC motor was used, and the motor output torque was also controlled by the PC. Braking conditions were fed back to the driver mainly by the visual display of the leading car. An additional cue to braking conditions was provided by controlling the pedal force exerted on the driver's foot.

4.1.1. Vehicle dynamics

The braking simulator used a simple two degree-of-freedom model for vehicle motion (Tabe *et al.*, 1985). Figure 11 shows the variables in the model developed for this simulator. The vehicle system consisted of a single wheel with mass M and moment of inertia I. The equations of motion based on above modeling are as follows:

$$M\dot{v} = F \quad (11)$$

Friction force on the wheel was modeled as a function of road surface condition and wheel slip:

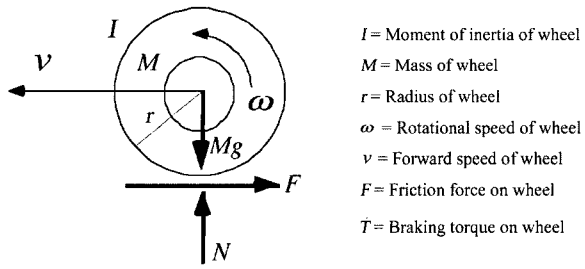

Figure 11. Two degree-of-freedom vehicle model.

$$F = \mu(\lambda)Mg \tag{12}$$

$$\lambda = \frac{v - r\omega}{v} \tag{13}$$

where μ = friction coefficient of road
λ = wheel slip ratio

4.1.2. Brake system dynamics

This brake system model employed by the braking simulator consisted of a vacuum booster, a master cylinder, a wheel cylinder, and a brake pad.

The relationship between pedal displacement and booster output force was modeled as a first order system as follows:

$$\frac{F}{X} = \frac{K_1}{\tau_1 s + 1} \tag{14}$$

where F = vacuum booster output force
X = brake pedal displacement

Brake system hydraulics between the master cylinder and the wheel cylinder were also modeled as a first order system (Tabe *et al.*, 1985):

$$\frac{P}{P^*} = \frac{K_2}{\tau_2 s + 1} \tag{15}$$

where P = brake pressure at wheel cylinder
P^* = pressure at master cylinder

The relationship between wheel cylinder pressure and brake torque was approximated to be linear:

$$T = Kp \tag{16}$$

where K = brake gain or brake effectiveness

For antilock brake systems, brake pressure was modulated depending on the wheel slip. This braking simulator used a simple logic of ABS activation: when the wheel slip exceeded a threshold, brake pressure was relieved. The ABS cycle in the driving simulator was around 10 Hz.

4.2. Test Models

Vehicle models with five different brake systems were tested using the brake simulator. The brake systems consisted of three conventional brake systems and the two new brake systems described in section 3. The test models used were as follows:

- Model 1

This model was a passenger car that was not equipped with an antilock brake system;

- Model 2

This model was a passenger car equipped with a conventional antilock brake system. Activation of the ABS was cued by vibration at the brake pedal;

- Model 3

This model was a passenger car equipped with an antilock brake system and servo system to control brake pedal stiffness. Stiffness of the brake pedal was softened 50% upon activation of the ABS instead of the vibration as in Model 2;

- Model 4

This model was a passenger car equipped with an antilock brake system and a road surface condition sensor. Upon detection of a wet/icy road surface, the stiffness of the brake pedal was reduced by 50%. This model assumed detection of road surface condition by a perfect sensor;

- Model 5

The last model was a passenger car equipped with an antilock brake system. While the ABS functioned normally, the vibration at the brake pedal was filtered out in this model.

4.3. Experimental Tasks

The performances of the five brake systems described above were tested using the driving simulator. Road condition awareness and situation adaptability of the drivers was evaluated under different braking situations and road surface conditions.

In the driving simulator, the driver followed one lead car at a speed of 100 km/h trying to keep a 2-second headway before the lead car, at a random time, braked to stop. The driver was able to control the speed of the driving car only through the brake pedal. In the experiment, the simulation produced various braking situations according to erratic behavior of the lead car and road conditions. In this case the drivers were instructed to follow the lead car and to react as they would in an actual driving situation. In the experiment, four situations were devised combining two different lead car behaviors and two different road surface conditions: gentle braking on a dry road, gentle braking on a wet/icy

road, emergency braking on a dry road, and emergency braking on a wet/icy road. The four situations appeared in random order.

In the experiments, the driver was asked to estimate the road surface condition and decide whether it was dry or wet/icy. The driver's estimates were rated on a five-point scale. The driver could choose one of five different responses: definitely dry, maybe dry, undeterminable, maybe wet/icy, and definitely wet/icy. The driver's estimates were scored as follows.

- Correct with certainty: +2 points
- Correct but without certainty: +1 point
- Indecisive: 0 point
- Incorrect with no certainty: –1 point
- Incorrect with no certainty: –2 point

For example, if the driver chose "maybe dry" as his response, while the actual road condition was wet, the score for his estimation was –1.

Also, the adaptability to four situations that randomly appeared was rated. In the emergency braking situation, the driver's task was to avoid rear-end collisions. In the gentle braking situation, the driver's task was to stop the car as close to the lead car as possible without collision. Either collision with the lead car or excessive braking in the gentle braking situation was considered to be a failure in situation adaptation. The rating system for the situation adaptation experiment is as follows:

- Gentle braking

(1) Distance to lead car when stopped < Initial headway:
Rate = 2×(1 – Distance to lead car when stopped/Initial headway)
(2) Distance to lead car when stopped > Initial headway:
Rate = 0

- Emergency braking

(1) No collision occurred:
Rate = 2
(2) Speed at collision < 48 km/h:
Rate = 2×(1-Speed at collision/48 km/h)
(3) Speed at collision > 48 km/h:
Rate = 0

Before the experiments, the drivers were first given oral and written instruction describing the brake system and the task of the experiments. They were then given unlimited practice sessions until they felt confident to manipulate the brake pedal in a variety of situations that would appear in actual experiments. The practice sessions were followed by the three different experiments described above. Each experiment was conducted for about 10 minutes with 5-minute breaks between them. A total of nine drivers voluntarily participated in the experiments. All the drivers were affiliated with MIT (all males, mean age of 25 years) with at least three years of driving experiences.

4.4. Results of Simulation Experiments

The performance of the five test models were compared in terms of the performance indices such as road condition awareness and situation adaptability.

Figure 12 illustrates typical phase plane plots, where pedal depression speed is plotted against pedal travel. These phase plane plots compare the driver's pedal maneuver on dry and wet/icy roads. Plots are presented for Models 2, 3 and 4, where pedal stiffness changes depending on road conditions. Among these three models, Model 4 indicates the largest phase plane difference for the two different road conditions; the area of the plot for the wet/icy road is much larger than that for the dry road. Model 3 shows a sudden change of pedal

Table 1. Characteristic parameters in phase plane plots on dry and wet/icy roads.

Model	Area		Peak depression		Peak depression speed	
	Dry	Wet/Icy	Dry	Wet/Icy	Dry	Wet/Icy
Model 2	3.430±0.862	3.123±0.589	0.984±0.071	1.002±0.089	5.392±1.170	5.259±0.988
	Mean difference	p-value	Mean difference	p-value	Mean difference	p-value
	0.307	0.5332	0.018	0.7376	0.133	0.8702
Model 3	3.849±0.463	3.591±0.320	1.142±0.055	1.203±0.015	3.085±0.504	4.316±0.269
	Mean difference	p-value	Mean difference	p-value	Mean difference	p-value
	0.258	0.3418	0.061	**0.03123**	1.231	**0.00006111**
Model 4	4.135±0.759	6.072±0.877	1.103±0.068	1.189±0.020	6.588±1.241	7.570±1.095
	Mean difference	p-value	Mean difference	p-value	Mean difference	p-value
	1.937	**0.001208**	0.086	**0.00004163**	0.982	0.2211

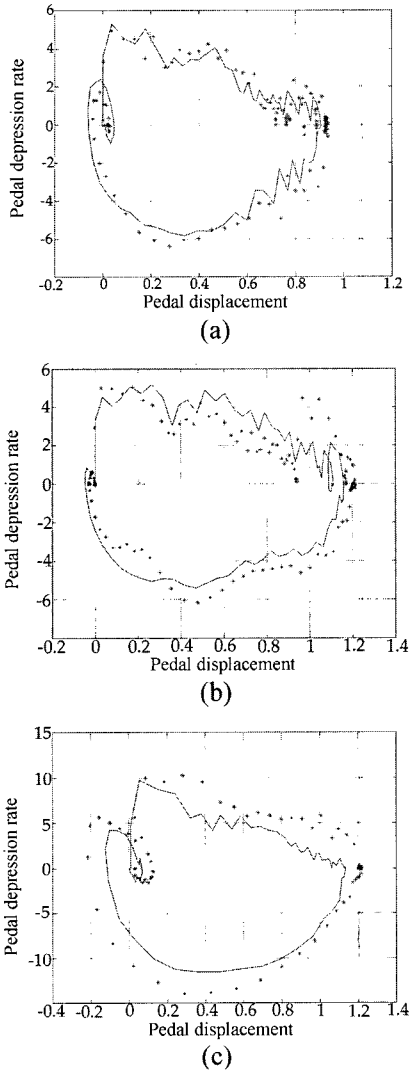

Figure 12. Normalized phase plane plots of brake pedal depression on dry and wet/icy roads: (a) Model 2; (b) Model 3; (c) Model 4. (solid line: dry road, dotted line: wet/icy road).

depression speed, which appears as a spike just before full braking in Figure 12. This indicates a sudden yielding of the pedal upon ABS activation. Model 2 indicates no substantial change in pedal depression on different road conditions. This phase plane plot provides a good format for comparing the driver's kinesthetic perception. Since neuromuscular systems provide sensing of muscle stretch and stretch rate (spindle afferent) as well as force sensing (Golgi tendon afferent), the brake pedals in Model 3 and 4 provided the driver with a kinesthetic display of braking or road condition.

The phase plane plots were characterized by their areas, peak pedal depressions, and peak pedal-depression speeds. The areas of the phase plane plots were taken to include only the region above the pedal-depression axis. The mean values and the associated 95% confidence intervals of the means (using Student's t-distribution) of the three characteristic parameters are presented for each driver with Models 2, 3, and 4 for dry and wet/icy roads in Table 1. The phase plane plots were drawn from data obtained from four drivers during the experiments. Unless otherwise noted in the table, four independent plots were estimated for each driver on each road condition. Statistically significant changes ($p<0.05$, Student's t-test) depending on road conditions are marked by bold face. Using an unpaired, two-tailed Student's t-test, the significance of changes in the phase plane plots for different road conditions were evaluated. For Model 2, no significant changes in the phase plane plots were observed for wet/icy road conditions. Model 3 showed significant increase in peak depression ($p=0.03123$, Student's t-test) and peak depression speed ($p=0.00006111$, Student's t-test) near full pedal depression under wet/icy road conditions. Model 4 exhibited significant increase in area ($p=0.001208$, Student's t-test) and peak depression ($p=0.00004163$, Student's t-test) on wet/icy road. Clearly, Models 3 and 4 appear to provide a kinesthetic display to the driver.

The drivers were questioned on road surface conditions perceived and reported immediately after each braking situation. The ratings of the road condition estimates from four drivers are listed in Figure 13. Each point represents the sum across all situations in the specified experiments. It is evident from the ratings that the drivers perceived road conditions easily in Models 3 and 4. While there were variations in baselines among the drivers, for each driver the ratings were considerably higher for Models 3 and 4. Especially in Model 4, the drivers recognized the road conditions correctly in most situations. This result can be explained by the discussion in the previous section about the driver's kinesthetic perception. Clearly, the change in phase-plane portrait of pedal depression appears to help the drivers perceive the road surface conditions.

From the situation adaptation experiment, the drivers' situation adaptation for each model was evaluated. The

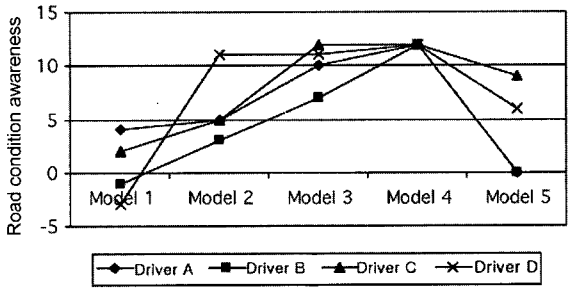

Figure 13. Road condition awareness results.

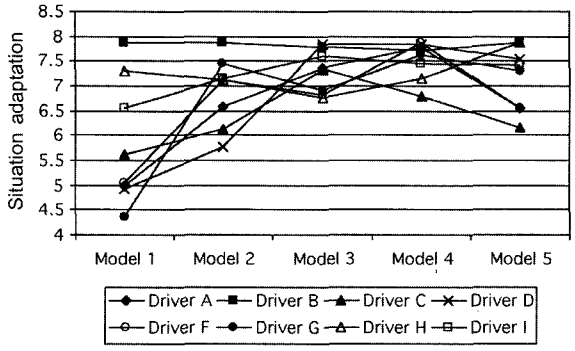

Figure 14. Situation adaptation results.

ratings of the situation adaptation from eight drivers are given in Figure 14. Each point represents the sum across all situations for each driver and model. Model 3 and Model 4 had high ratings with small variations among the drivers. Model 1 showed the largest variation among drivers.

The drivers appeared to perceive the road conditions more accurately under the proposed designs (Models 3 and 4). Also, the proposed designs appeared to help the driver's situation adaptability in various braking situations.

5. DISCUSSION

In braking the driver depends on his senses (visual, vestibular, auditory, etc.) to receive information about on-going traffic, and his task is to manipulate the brake pedal in order to stop his vehicle according to on-going traffic. To produce a desired pedal displacement the driver must produce a force determined by the mechanical stiffness or impedance of the brake pedal; to produce a desired force requires a particular displacement, also determined by the impedance. The impedance characteristic of the brake pedal has a strong effect on the driver's braking performance.

Control input device should be designed so that it serves as a tactile-kinesthetic display of output as well as an input device and provides better dynamic compatibility between system output and the operator's response. However, currently the brake pedal is not designed to display the braking performance, but rather is only a simple input device. While ABS takes full advantage of the brake control capabilities available with modern electronic, the human-machine interface for the ABS has not been designed to fully utilize the advanced features of the brake system. Pulsing at the brake pedal only indicates ABS activation; this signal does not serve as an intuitive cue of braking performance since vibration is commonly used as a warning or an indicator of malfunction of a system.

In teleoperation studies, adaptive impedance at a master port and at a slave port is known to improve the performance of a contact task (Raju, 1988). In this study, BBW system is considered to be a type of teleoperator performing a contact task. The goal of this study was to exploit new aspects in designing brake pedal feel that provide the driver with intuitive brake control and proper performance information. Based on teleoperation concepts, this paper developed two new brake systems. The new designs account for the characteristics of human leg motion and kinesthetic feedback to the driver. The potential effectiveness of the proposed designs was confirmed through the driving simulation.

6. CONCLUSIONS

While there is no analytical (or objective) standard in evaluating or designing brake pedal feel, common ground may be drawn by investigating dynamic characteristics of brake systems and the human driver. This study attempted to provide guidelines in brake pedal feel design. This study suggests the followings in designing a brake pedal.

(1) Based on mathematical models of brake system, brake pedal feel can be characterized by its impedance. The impedance can be represented by impedance surface, which formulate pedal force as a function of pedal stroke and its time rate.
(2) The mechanisms underlying drivers' maneuver of the brake pedal should be taken into consideration in designing the brake pedal feel.
(3) BBW system can be designed to serve as a teleoperator, which provides the driver with kinesthetic feedback of braking conditions or performance.
(4) From the simulator tests, it is shown that change of pedal impedance has a great effect on braking performance.
(5) Two new brake systems proposed in this study can help the driver perceive the road conditions through kinesthetic cue from the brake pedal. The system performance of driver-vehicle system was improved by enhancing the driver's road condition awareness.

ACKNOWLEDGEMENT–The author would like to thank all the experimental subjects for their participation in this study.

REFERENCES

Barfield, W. and Furness, T. (1995). *Virtual Environments and Advanced Interface Design*. Oxford: Oxford Univ. Press.

Ciamberlini, C., Innocenti, G. and Longobardi, G. (1995). *Review of Scientific Instruments*, **66**, 2684–2689.

Dairou, V., Priez, A., Sieffermann, J-M. and Danzart, M. (2003). An original method to predict brake feel: A combination of design of experiments and sensory

science. *SAE Paper No.* 2003-01-0598.

Ebert, D. and Kaatz, R. (1994). Objective characterization of vehicle brake feel. *SAE Paper No.* 940331.

Gerdes, J. and Hedrick, J. (1999). Brake system modeling for simulation and control. *ASME J. of Dynamic Systems, Measurement and Control* **121**, 3, 496–503.

Hertz, E., Hilton, J. and Johnson, D. (1995). An analysis of the crash experience of passenger cars equipped with antilock braking systems. *U.S. Department of Transportation, NHTSA*, DOT HS 808279.

Kelling, N. and Leteinturier, P. (2003). X-by-wire: opportunities, challenges and trends. *SAE Paper No.* 2003-01-0113.

Jackson, D. (1997). *Development of Full-body Models for Human Jump Landing Dynamics and Control.* Ph.D. Dissertation. Department of Aeronautics and Astronautics. Massachusetts Institute of Technology. Cambridge. MA, USA.

Park, S. (1999). *Driver-vehicle Interaction in Braking.* Ph.D. Dissertation. Department of Mechanical Engineering. Massachusetts Institute of Technology. Cambridge, MA, USA.

Raju, G. (1988). *Operator Adjustable Impedance in Bilateral Remote Manipulation.* Ph.D. Dissertation. Department of Mechanical Engineering. *Massachusetts Institute of Technology.* Cambridge, MA, USA.

Sato, H., Sugiura, A., Oshima, M. and Doi, S. (1996). Numericalization of vehicle brake feel – Vehicle brake feel modeling by neural network. *SAE Paper No.* 968431.

Tabe, T., Ohka, N., Kuraoka, H. and Ohba, M. (1985). Automotive antiskid system using modern control theory. *Proc. IEEE IECON'85*, 390–395.

Yamaguchi, J. (1997). Tech briefs - Brake assist systems. *Automotive Engineering Magazine*, June, 53–54.

Won, J. and Hogan, N. (1995). Stability properties of human reaching movements. *Experimental Brain Research*, **107**, 125–36.

Yu, F., Feng, J.-Z. and Li, J. (2002). A fuzzy logic controller for vehicle ABS with a on-line optimized target wheel slip ratio. *Int. J. Automotive Technology* **3**, **4**, 165–170.